Unsteady MHD stagnation-point flow with heat and mass transfer for a three-dimensional porous body in the presence of heat generation/absorption and chemical reaction

Ali J. Chamkha*

Manufacturing Engineering Department,
The Public Authority for Applied
Education and Training, Shuweikh 70654, Kuwait
E-mail: achamkha@yahoo.com
*Corresponding author

Sameh E. Ahmed

Faculty of Sciences, Department of Mathematics,
South Valley University, Qena, Egypt
E-mail: sameh_sci_math@yahoo.com

Abstract: The problem of unsteady Magnetohydrodynamic (MHD) flow with heat and mass transfer near the stagnation point of a three-dimensional (3D) porous body in the presence of heat source/sink and chemical reaction effect has been studied numerically using an efficient iterative implicit finite-difference method. The numerical results are validated by favourable comparisons with previously published work. Three forms for the free stream velocity distributions namely a constantly accelerating flow, a periodic fluctuating flow and an exponentially decelerating flow are considered. Numerical results for the velocity components in the *x*-and *y*-directions, temperature distribution and concentration distribution as well as the skin-friction coefficients and the Nusselt and Sherwood numbers are presented graphically for various parametric conditions and discussed.

Keywords: mixed convection; three-dimensional flow; stagnation point; heat source/sink; chemical reaction.

Biographical notes: Ali J. Chamkha is a Professor in the Manufacturing Engineering Department, College of Technological Studies at the Public Authority for Applied Education and Training in Kuwait. He earned his PhD in Mechanical Engineering from Tennessee Technological University, USA, in 1989. His research interests include multiphase fluid-particle dynamics, fluid flow in porous media, heat and mass transfer, magnetohydrodynamics and fluid-particle separation. He has served as an Associate Editor for *Fluid/Particle Separation Journal* and *International Journal of Energy & Technology*. He has authored and co-authored over 300 papers in archival journals and conferences.

Sameh E. Ahmed earned his MSc in Applied Mathematics (Fluid Mechanics). He is a member in Mathematics Department, Faculty of Science, South Valley University, Egypt. His research interests include heat and mass transfer, computational fluid dynamics and nanofluid mechanics. He has published several papers in archival journals (*Transport in Porous Media*, *Meccanica*, *Heat and Mass Transfer*, *International Communications in Heat and Mass Transfer*, *Non-linear Analysis Modelling and Control* and others). Now, he is preparing his PhD thesis.

1 Introduction

The motivation of studying transient free and mixed convection flows in the stagnation-point region of a body is due to the fact that the heat transfer is maximum at the stagnation point and unsteadiness in the flow field can be caused either by a sudden change in the wall temperature or by a time-dependent wall temperature. It may be remarked that even though the stagnation-point solutions are valid in a small region in the vicinity of the stagnation point of a 3D body, they represent several physical flows of engineering

significance (Slaouti et al., 1998). 3D mixed convection boundary-layer flows appear to have received (to the authors' knowledge) relatively little attention in the literature for more than a decade in comparison with their axi-symmetric two-dimensional (2D) counterparts although in most engineering practices, flows are more likely to be 3D in nature than not. The difficulty encountered in studying such flows may somewhat be alleviated in considering examples tenable to analyses with a view to providing a deeper insight into the more complex flow situations. In this spirit, Yao and Catton (1977) considered the laminar boundary layer over a heated hollow semi-infinite cylinder with its axis aligned parallel to a uniform stream and normal to the direction of gravity. An interesting example of 3D mixed convection is given by the work of Eichhorn and Hasan (1980) where the buoyancy force acts in a direction perpendicular to that of a free stream flowing past a wedge. Ridha (1990) has studied mixed convection in a streamwise corner and have looked into the simpler case with asymptotic suction when the corner line is kept vertical; this offered the possibility to obtain exact solutions for the Navier–Stokes and energy equations. The 3D mixed convection boundary-layer flow over a vertical surface near a plane of symmetry was considered by Ridha (1996) and the corresponding similarity equations were found to be non-unique. Four solutions were obtained for some situations. Usually, it is convenient to seek self-similar solutions or approximate perturbation ones based on already existing similarity ones; these solutions would help to provide approximate correlation formulae for engineering use. These solutions provide intermediate asymptotics (Barenblatt and Zel'dovich, 1972). However, in practice, it is more desirable to have non-similar solutions to bring out more fully the effect of buoyancy force on forced convection.

The problem of boundary-layer free convection of a viscous fluid in the vicinity of a 3D stagnation point on surfaces has been the object of several studies in the past. Davey (1961) has studied the problem of boundary-layer flow at a saddle point of attachment. Papenfuss (1974a, 1974b, 1977a, 1977b) has studied the steady laminar incompressible and compressible 3D stagnation-point second-order boundary-layer flow with or without mass transfer in the nodal point region. Kumari (1988a, 1988b) has considered second-order boundary-layer effects for the unsteady laminar incompressible and compressible 3D stagnation-point flow. The boundary-layer 3D flow near a stagnation point was discussed by Howarth (1951). Jeng and Williams (1973) have investigated the transpiration cooling in 3D laminar boundary-layer flows near a stagnation point. The steady, laminar incompressible 3D stagnation-point flow with large injection rates has been studied by Walton (1973) using the method of matched asymptotic expansion. Krishnaswamy and Nath (1982) have studied the effect of large injection rates on the steady, laminar compressible 3D stagnation-point flow using an implicit finite-difference scheme. Kumari and Nath (1984) have considered the unsteady free convection flow in the stagnation-point region

of a heated porous 3D body where the unsteadiness in the flow field was caused by a time-dependent wall temperature. The semi-similar equations governing the flow were solved numerically using an implicit finite-difference scheme. Vasantha and Nath (1986a, 1986b) have extended the work of Krishnaswamy and Nath (1982) to the unsteady case by obtaining both semi-similar (Vasantha and Nath, 1986a) and locally self-similar (Vasantha and Nath, 1986b) solutions. The similarity solution for unsteady incompressible 3D stagnation-point flow in the nodal point region with hard blowing has been presented by Prasad and Rajappa (1981) using an approximate method. Slaouti et al. (1998) have studied unsteady free convection flow in the stagnation-point region of a 3D body. The effect of large injection rates on unsteady mixed convection flow at a 3D stagnation point was investigated by Eswara and Nath (1999). Most recently, Shafie et al. (2007) have considered g-Jitter free convection flow in the stagnation-point region of a 3D body. Xu et al. (2008) have reported series solutions for unsteady free convection flow in the stagnation-point region of a 3D body using the Homotopy Analysis Method (HAM) method.

There has been a renewed interest in studying MHD flow and heat transfer owing to the effect of magnetic fields on the boundary-layer flow control and on the performance of many systems using electrically conducting fluids. In addition, this type of flow has attracted the interest of many investigators in view of its applications in many engineering problems such as MHD generators, plasma studies, nuclear reactors and geothermal energy extractions. Bhattacharyya and Gupta (1998) have studied MHD flow and heat transfer at a general 3D stagnation point. Ishak et al. (2008) have considered MHD flow of a micropolar fluid towards a stagnation point on a vertical surface. Rahman and Salahuddin (2010) discussed MHD heat and mass transfer flow along a radiate isothermal inclined surface with the effects of variable electric conductivity and temperature-dependent viscosity. The effects of variable electric conductivity and non-uniform heat source (or sink) on convective micropolar fluid flow along an inclined flat plate with surface heat flux were studied by Rahman et al. (2009).

In many chemical engineering processes, chemical reactions take place between a foreign mass and the working fluid. The order of the chemical reactions depends on several factors. One of the simplest chemical reactions is the first-order homogeneous reaction in which the rate of reaction is directly proportional to the species concentration. Also, in certain industrial problems dealing with chemical reactions and dissociating fluids, heat generation/absorption and chemical reaction effects become important (Vajravelu and Nayfeh, 1992). Anjali Devi and Kandasamy (2002) have studied the effects of chemical reaction, heat and mass transfer on non-linear MHD laminar boundary-layer flow over a wedge with suction and injection. Sharma and Singh (2009) reported on the effects of variable thermal conductivity and heat source/sink on MHD flow near a stagnation point on a linearly stretching sheet. Chamkha

(1999) has reported on hydromagnetic 3D free convection on a vertical stretching surface with heat generation or absorption. Recently, Rahman and Al-Lawatia (2010) have reported on the effects of higher-order chemical reaction on micropolar fluid flow for a power-law stretched permeable sheet in a porous media with variable wall concentration.

The objective of this paper is to generalise the problem of Eswara and Nath (1999) by including heat and mass transfer, magnetic field force, heat generation/absorption and chemical reaction effects. An efficient, iterative, tri-diagonal implicit finite-difference method is used to solve the transformed non-similar conservation boundary-layer equations. The obtained results are presented graphically to illustrate the influences of different physical parameters on the velocity components, temperature distributions, concentration distributions, skin-friction coefficients, Nusselt and Sherwood numbers.

2 Governing equations

Consider the unsteady laminar incompressible boundary-layer flow of a viscous electrically conducting fluid at a 3D stagnation point with magnetic field, chemical reaction, heat generation/absorption and suction/injection effects. A uniform transverse magnetic field normal to the body surface is assumed to be applied. The fluid properties are assumed to be constant and the chemical reaction is taking place in the flow. The velocity components of the inviscid flow over the 3D body surface are given by:

$$zdu_e(x,t) = ax\phi(\tau), \quad v_e(x,t) = by\phi(\tau). \tag{1}$$

It is assumed that near the stagnation point, the free stream temperature is constant and viscous and magnetic dissipation effects are negligible. Notice that for $T_w > T_\infty$ the buoyancy force, which arises due to temperature differences, will aid the forced flow. On the other hand, if $T_w < T_\infty$, the resulting buoyancy force will oppose the forced flow. Under these assumptions as well as the Boussinesq approximation, the continuity, momentum, energy and concentration equations are given by

$$\frac{\partial u}{\partial x} + \frac{\partial v}{\partial y} + \frac{\partial w}{\partial z} = 0, \tag{2}$$

$$\frac{\partial u}{\partial t} + u\frac{\partial u}{\partial x} + v\frac{\partial u}{\partial y} + w\frac{\partial u}{\partial z} = \frac{\partial u_e}{\partial t}$$
$$+ u_e\frac{\partial u_e}{\partial x} + \upsilon\frac{\partial^2 u}{\partial z^2} - \frac{\sigma\beta_0^2}{\rho}(u - u_e)$$
$$+ \left[g\beta(T - T_\infty) + g\beta_c(C - C_\infty)\right]x/L, \tag{3}$$

$$\frac{\partial v}{\partial t} + u\frac{\partial v}{\partial x} + v\frac{\partial v}{\partial y} + w\frac{\partial v}{\partial z} = \frac{\partial v_e}{\partial t}$$
$$+ v_e\frac{\partial v_e}{\partial y} + \upsilon\frac{\partial^2 v}{\partial z^2} - \frac{\sigma\beta_0^2}{\rho}(v - v_e)$$
$$+ \left[g\beta(T - T_\infty) + g\beta_c(C - C_\infty)\right]cy/L, \tag{4}$$

$$\frac{\partial T}{\partial t} + u\frac{\partial T}{\partial x} + v\frac{\partial T}{\partial y} + w\frac{\partial T}{\partial z} = \frac{k}{\rho C_p}\frac{\partial^2 T}{\partial z^2} + \frac{Q_0}{\rho C_p}(T - T_\infty), \tag{5}$$

$$\frac{\partial C}{\partial t} + u\frac{\partial C}{\partial x} + v\frac{\partial C}{\partial y} + w\frac{\partial C}{\partial z} = D\frac{\partial^2 C}{\partial y^2} - k_c(C - C_\infty). \tag{6}$$

The initial and boundary conditions are

$$t = 0 : u(x,y,z,t) = u_i(x,y,z), v(x,y,z,t)$$
$$= v_i(x,y,z), w(x,y,z,t) = w_i(x,y,z), T(x,y,z,t)$$
$$= T_i(x,y,z), C(x,y,z,t) = C_i(x,y,z),$$
$$t > 0 : u(x,y,z,t) = 0, v(x,y,z,t) = 0, w(x,y,z,t)$$
$$= w_w, T(x,y,z,t) = T_w, C(x,y,z,t) = C_w \text{ at } y = 0,$$
$$t > 0 : u(x,y,z,t) = u_e(x,y), v(x,y,z,t)$$
$$= v_e(x,y), T(x,y,z,t)$$
$$= T_\infty, C(x,y,z,t) = C_\infty \text{ as } y \to \infty. \tag{7}$$

3 Non-similar solution

By considering the following dimensionless transformation

$$\eta = z(a/\upsilon)^{1/2}, \tau = at, u = ax\phi(\tau)F'(\eta,\tau),$$
$$v = by\phi(\tau)S'(\eta,\tau),$$
$$w = -\sqrt{a\upsilon}(F + cS)\phi(\tau), \theta(\eta,\tau) \tag{8}$$
$$= \frac{T - T_\infty}{T_w - T_\infty}, \Phi(\eta,\tau) = \frac{C - C_\infty}{C_w - C_\infty}, c = b/a.$$

Equations (3)–(6) are converted to

$$\frac{\partial^3 F}{\partial\eta^3} + \phi(F + cS)\frac{\partial^2 F}{\partial\eta^2} + \phi\left[1 - \left(\frac{\partial F}{\partial\eta}\right)^2\right]$$
$$+ \phi^{-1}(\lambda_1\theta + \lambda_2\Phi) + \left(1 - \frac{\partial F}{\partial\eta}\right)\left(M + \phi^{-1}\frac{d\phi}{d\tau}\right) - \frac{\partial^2 F}{\partial\eta\partial\tau} = 0, \tag{9}$$

$$\frac{\partial^3 S}{\partial\eta^3} + \phi(F + cS)\frac{\partial^2 S}{\partial\eta^2} + c\phi\left[1 - \left(\frac{\partial S}{\partial\eta}\right)^2\right]$$
$$+ \phi^{-1}(\lambda_1\theta + \lambda_2\Phi) + \left(1 - \frac{\partial S}{\partial\eta}\right)\left(M + \phi^{-1}\frac{d\phi}{d\tau}\right) - \frac{\partial^2 S}{\partial\eta\partial\tau} = 0, \tag{10}$$

$$\frac{1}{\Pr}\frac{\partial^2\theta}{\partial\eta^2} + \phi(F + cS)\frac{\partial\theta}{\partial\eta} + \delta\theta - \frac{\partial\theta}{\partial\tau} = 0, \tag{11}$$

$$\frac{1}{Sc}\frac{\partial^2\Phi}{\partial\eta^2} + \phi(F + cS)\frac{\partial\Phi}{\partial\eta} - \gamma\Phi - \frac{\partial\Phi}{\partial\tau} = 0 \tag{12}$$

where $\Pr = \mu C_p/k$ is the Prandtl number, $Gr = g\beta L^3(T_w - T_\infty)/\upsilon^2$ is the Grashof number, $Gr_c = g\beta_c L^3(T_w - T_\infty)/\upsilon^2$ is the modified Grashof number, $\mathrm{Re}_L = aL^2/\upsilon$ is Reynolds number, $(\lambda_1 = Gr/\mathrm{Re}_L^2, \lambda_2 = Gr_C/\mathrm{Re}_L^2)$ is the buoyancy parameters, $Sc = \upsilon/D$ is the Schmidt number, $M = \sigma\beta_0^2/\rho a$ is the magnetic field parameter, $\delta = Q_0/\rho C_p a$ is the heat generation/absorption parameter and $\gamma = k_c/a$ is the chemical reaction parameter.

The transformed dimensionless boundary conditions (7) reduce to

$$\eta = 0 : \frac{\partial F}{\partial \eta} = \frac{\partial S}{\partial \eta} = 0, \, F = -f_w, \, \theta = 1, \, \Phi = 1,$$

$$\eta \to \infty : \frac{\partial F}{\partial \eta} = \frac{\partial S}{\partial \eta} = 1, \, \theta = 0, \, \Phi = 0. \tag{13}$$

In the above-mentioned equation, $f_w = (w_w / u_e)\sqrt{\mathrm{Re}_x}$ is the suction/injection parameter and $f_w > 0$ or $f_w < 0$ according to whether there is a suction or injection, respectively. In this study, we will consider three forms of the free stream velocity distributions:

- a constantly accelerating flow given by $\phi(\tau) = 1 + \varepsilon \tau^2$

- a periodic fluctuating flow represented by
  $\phi(\tau) = (1 + \varepsilon_1 \cos \omega \tau)/(1 + \varepsilon_1)$

- an exponentially decelerating flow
  $\phi(\tau) = 1 - \varepsilon_2[1 - \exp(-\varepsilon_3 \tau^2)].$

Furthermore, the initial velocities, temperature and concentration at $\tau = 0$ are given by the steady flow equations, obtained by putting $\phi(\tau) = 1$, $\phi_\tau = F_{\eta\tau} = S_{\eta\tau} = \theta_\tau = \Phi_\tau = 0$ in Equations (9)–(12).

The most important results for this problem are the local skin-friction coefficients in the x- and y-directions, local rate of heat transfer at the wall in terms of Nusselt number and the local rate of mass transfer at the wall in terms of Sherwood number, which can be given by, respectively,

$$C_{Fx}(\mathrm{Re}_x)^{1/2} = 2\phi(\tau)\frac{\partial^2 F}{\partial \eta^2}\bigg|_{\eta=0},$$

where,

$$C_{Fx} = \frac{2}{\rho u_e^2}\left[\mu \frac{\partial u}{\partial z}\right]_{z=0}. \tag{14}$$

$$C_{Fy}(\mathrm{Re}_x)^{1/2} = 2(u_e / v_e)\phi(\tau)\frac{\partial^2 S}{\partial \eta^2}\bigg|_{\eta=0},$$

where,

$$C_{Fy} = \frac{2}{\rho v_e^2}\left[\mu \frac{\partial v}{\partial z}\right]_{z=0}. \tag{15}$$

$$(\mathrm{Re}_x)^{-1/2} Nu_x = -\frac{\partial \theta}{\partial \eta}\bigg|_{\eta=0},$$

where,

$$\mathrm{Nu}_x = -\frac{x}{T_w - T_\infty}\frac{\partial T}{\partial z}\bigg|_{z=0}, \tag{16}$$

$$(\mathrm{Re}_x)^{-1/2} Sh_x = -\frac{\partial \Phi}{\partial \eta}\bigg|_{\eta=0},$$

where,

$$\mathrm{Sh}_x = -\frac{x}{C_w - C_\infty}\frac{\partial C}{\partial z}\bigg|_{z=0}. \tag{17}$$

4 Numerical method

The system of Equations (9)–(12) with the boundary conditions (13) is solved numerically by means of an efficient, iterative, tri-diagonal implicit finite-difference method discussed previously by Blottner (1970). Equations (9)–(12) are discretised using three-point central difference formulae with f' replaced by another variable V. The η direction is divided into 196 nodal points and a variable step size is used to account for the sharp changes in the variables in the region close to the surface where viscous effects dominate. The initial step size used is $\Delta \eta_1 = 0.001$ and the growth factor $K = 1/037$ such that $\Delta \eta_n = K\Delta \eta_{n-1}$ (where the subscript n is the number of nodes minus one). This gives $\eta_{max} \approx 35$, which represents the edge of the boundary layer at infinity. The ordinary differential equations are then converted into linear algebraic equations that are solved by the Thomas algorithm discussed by Blottner (1970). Iteration is employed to deal with the non-linear nature of the governing equations. The convergence criterion employed in this work was based on the relative difference between the current and the previous iterations. When this difference or error reached 10^{-5}, then the solution was assumed converged and the iteration process was terminated.

To check the accuracy of the numerical method, the skin-friction parameters for the steady-state case is compared with those reported earlier by Eswara and Nath (1999), Howarth (1951), Davey (1961) and Jeng and Williams (1973) in the absence of the effects of magnetic field, heat generation/absorption, chemical reaction, buoyancy and suction/injection effects. As shown in Table 1, the present results are found to be in excellent agreement with the results of Eswara and Nath (1999), Howarth (1951), Davey (1961) and Jeng and Williams (1973). This favourable comparison lends confidence in the numerical results to be reported subsequently.

Table 1 Comparison of the skin-friction parameters for the steady-state case when $\lambda_1 = \lambda_2 = M = \delta = \gamma = f_w = 0$ (continues on next page)

| | *Eswara and Nath (1999)* | | *Davey (1961) and Howarth (1951)* | | *Jeng and Williams (1973)* | | *Present work* | |
C	$\partial^2 F/\partial \eta^2$	$\partial^2 S/\partial \eta^2$	$\partial^2 F/\partial \eta^2$	$\partial^2 S/\partial \eta^2$	$\partial^2 F/\partial \eta^2$	$\partial^2 S/\partial \eta^2$	$\partial^2 F/\partial \eta^2$	$\partial^2 S/\partial \eta^2$
1.00	1.3128	1.3128	1.3120	1.3120	1.3119	1.3119	1.3122	1.3122
0.75	1.2885	1.1642	1.2880	1.1640	1.2887	1.1643	1.2888	1.1646
0.50	1.2677	0.9980	1.2670	0.9980	1.2669	0.9981	1.2670	0.9983

Table 1   Comparison of the skin-friction parameters for the steady-state case when $\lambda_1 = \lambda_2 = M = \delta = \gamma = f_w = 0$ (continued)

| | *Eswara and Nath* (1999) | | *Davey* (1961) *and Howarth* (1951) | | *Jeng and Williams* (1973) | | *Present work* | |
| | $\partial^2 F/\partial \eta^2$ | $\partial^2 S/\partial \eta^2$ | $\partial^2 F/\partial \eta^2$ | $\partial^2 S/\partial \eta^2$ | $\partial^2 F/\partial \eta^2$ | $\partial^2 S/\partial \eta^2$ | $\partial^2 F/\partial \eta^2$ | $\partial^2 S/\partial \eta^2$ |
C								
0.25	1.2475	0.8050	1.2470	0.8050	1.2476	0.8051	1.2478	0.8050
0.00	1.2324	0.5706	1.2326	0.5705	1.2326	0.5705	1.2327	0.5707
−0.25	1.2249	0.2671	1.2251	0.2680	–	–	1.2253	0.2684
−0.50	1.2302	−0.1110	1.2302	−0.1115	–	–	1.2303	−0.1105
−0.75	1.2489	−0.4975	1.2473	−0.4821	–	–	1.2474	−0.4802

5   Results and discussion

Numerical computations are carried out and a parametric study is performed to illustrate the influence of the physical parameters on the velocity components in *x*- and *y*-direction, temperature and concentration profiles as well as the skin-friction coefficients and Nusselt and Sherwood numbers. The results of this parametric study are shown in Figures 1–18. In all of the obtained results, we fixed the values of the parameters ε, ε_1, ε_2 and ε_3 at 1.0, 0.1, 1.0 and 0.5, respectively.

Figure 1   Effect of suction/injection parameter on velocity components when $\phi(\tau) = 1 + \varepsilon\tau^2$
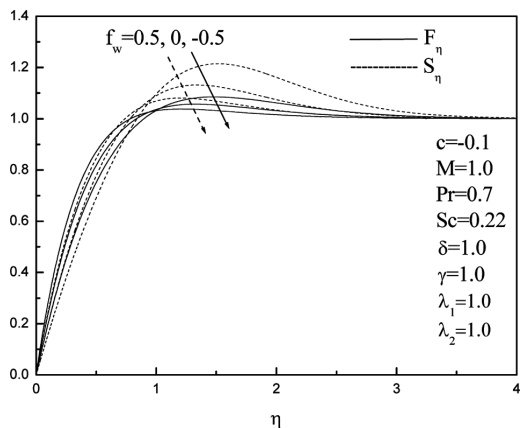

Figure 2   Effect of suction/injection parameter on temperature and concentration profiles when $\phi(\tau) = 1 + \varepsilon\tau^2$
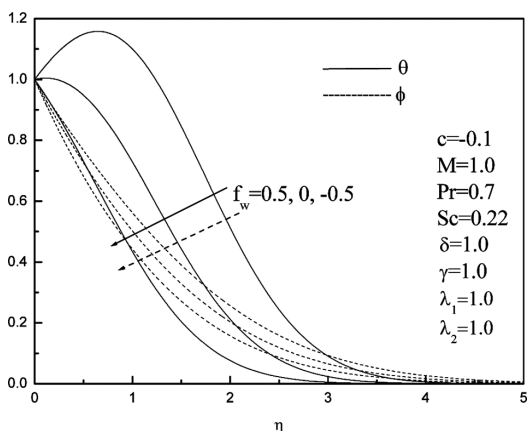

Figure 3   Effect of suction/injection parameter on skin-friction coefficients when $\phi(\tau) = 1 + \varepsilon\tau^2$
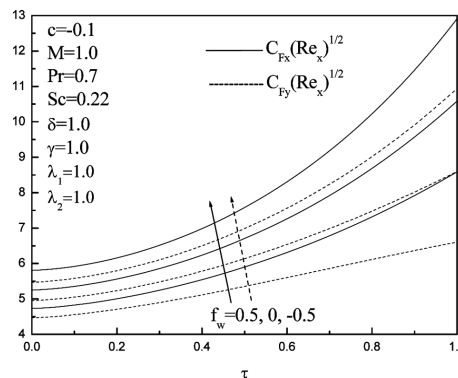

Figure 4   Effect of suction/injection parameter on Nusselt and Sherwood numbers when $\phi(\tau) = 1 + \varepsilon\tau^2$
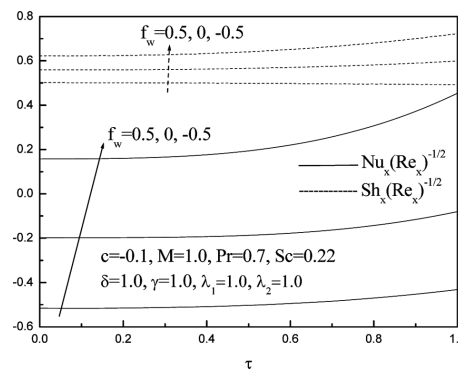

Figure 5   Effect of magnetic field parameter on velocity components when $\phi(\tau) = (1 + \varepsilon_1 \cos\omega\tau)/(1 + \varepsilon_1)$
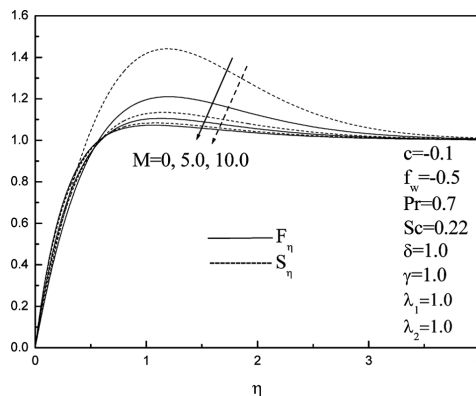
Figure 6 Effect of magnetic field parameter on skin-friction coefficients when $\phi(\tau) = (1 + \varepsilon_1 \cos\omega\tau)/(1 + \varepsilon_1)$
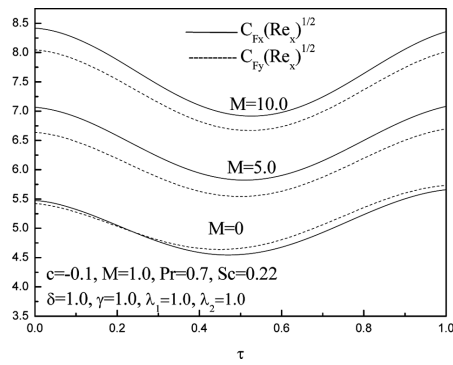

Figure 7 Effect of chemical reaction parameter on velocity components when $\phi(\tau) = 1 - \varepsilon_2[1 - \exp(-\varepsilon_3\tau^2)]$
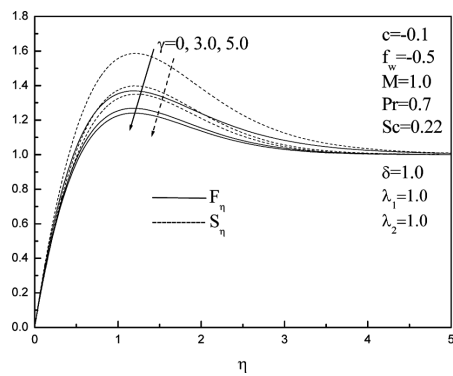

Figure 8 Effect of chemical reaction parameter on temperature and concentration profiles when $\phi(\tau) = 1 - \varepsilon_2[1 - \exp(-\varepsilon_3\tau^2)]$
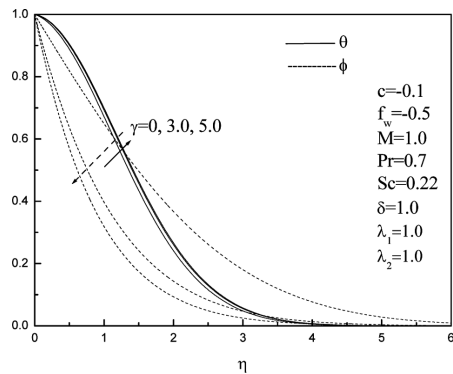

Figure 9 Effect of chemical reaction parameter on skin-friction coefficients when $\phi(\tau) = 1 - \varepsilon_2[1 - \exp(-\varepsilon_3\tau^2)]$
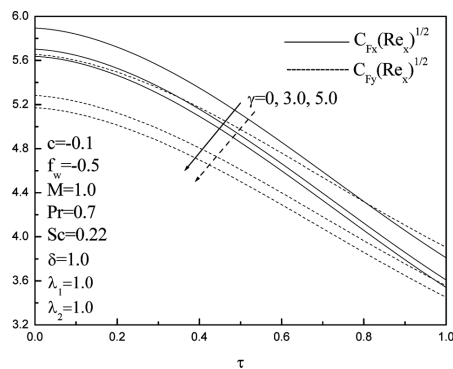

Figure 10 Effect of chemical reaction parameter on Nusselt and Sherwood numbers when $\phi(\tau) = 1 + \varepsilon_2[1 - \exp(-\varepsilon_3\tau^2)]$
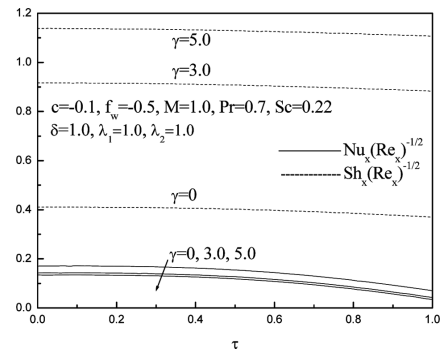

Figure 11 Effect of ratio of velocity gradients at the edge of the boundary layer on velocity components when $\phi(\tau) = (1 + \varepsilon_1 \cos\omega\tau)/(1 + \varepsilon_1)$
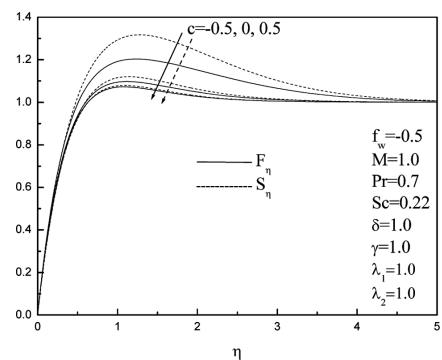

Figure 12 Effect of ratio of velocity gradients at the edge of the boundary layer on temperature and concentration profiles when $\phi(\tau) = (1 + \varepsilon_1 \cos\omega\tau)/(1 + \varepsilon_1)$
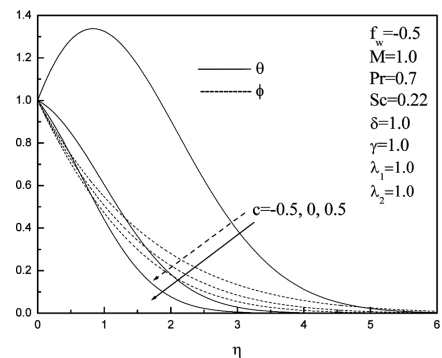

Figure 13 Effect of ratio of velocity gradients at the edge of the boundary layer on skin-friction coefficients when $\phi(\tau) = (1 + \varepsilon_1 \cos\omega\tau)/(1 + \varepsilon_1)$
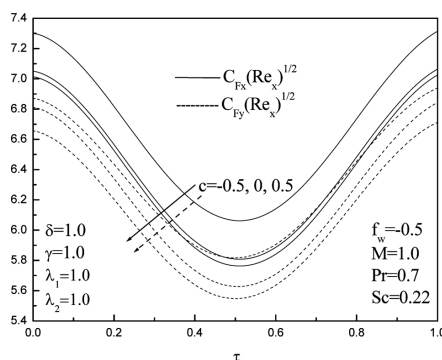
Figure 14 Effect of ratio of velocity gradients at the edge of the boundary layer on Nusselt and Sherwood numbers when $\phi(\tau) = (1 + \varepsilon_1 \cos \omega \tau)/(1 + \varepsilon_1)$
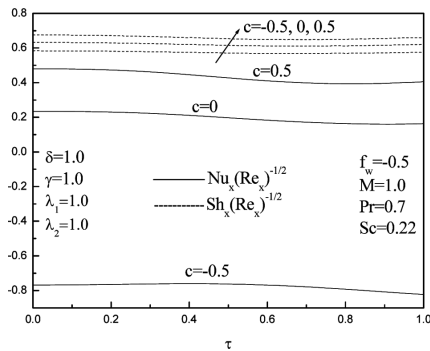

Figure 15 Effect of heat generation parameter on velocity components when $\phi(\tau) = (1 + \varepsilon_1 \cos \omega \tau)/(1 + \varepsilon_1)$
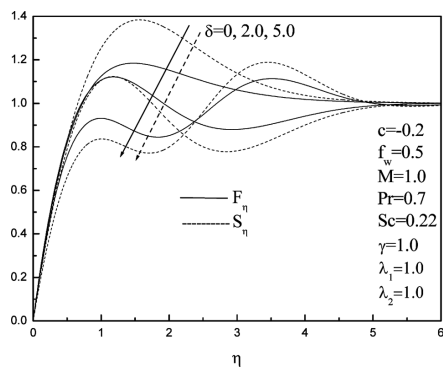

Figure 16 Effect of heat generation parameter on temperature and concentration profiles when $\phi(\tau) = (1 + \varepsilon_1 \cos \omega \tau)/(1 + \varepsilon_1)$
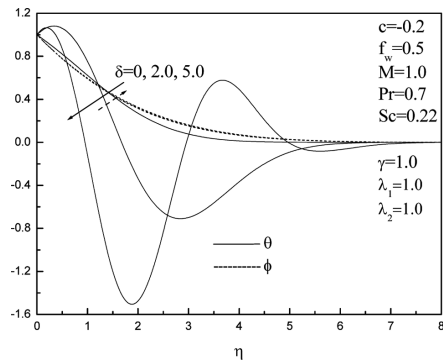

Figure 17 Effect of heat generation parameter on skin-friction coefficients when $\phi(\tau) = (1 + \varepsilon_1 \cos \omega \tau)/(1 + \varepsilon_1)$
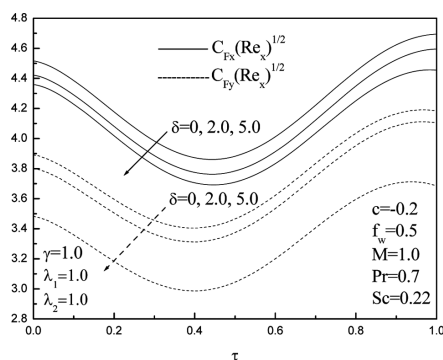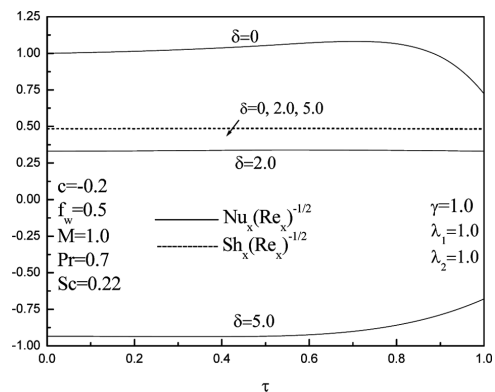

Figure 18 Effect of heat generation parameter on Nusselt and Sherwood numbers when $\phi(\tau) = (1 + \varepsilon_1 \cos \omega \tau)/(1 + \varepsilon_1)$

Figures 1–4 show the effects of the suction/injection parameter f_w on the velocity components in x- and y-directions, temperature profiles, concentration profiles, skin-friction coefficients and the Nusselt and Sherwood numbers for the case of a constantly accelerating flow for which the free stream velocity distribution is given by $\phi(\tau) = 1 + \varepsilon \tau^2$. It is clear from these figures that, as the suction/injection parameter increases, the velocity components decrease beside the wall and take an inverse behaviour after some distance from the wall. Also, increasing the value of the transpiration parameter leads to increases in both the temperature and the concentration distributions. However, the skin-friction coefficients, Nusselt number and the Sherwood number decrease with increasing values of the transpiration parameter f_w. In addition, since the function that represents the free stream velocity distribution namely $\phi(\tau)$ appears explicitly in Equations (14) and (15) for the definitions of the skin-friction coefficients $C_{Fx}(\mathrm{Re}_x)^{1/2}$ and $C_{Fy}(\mathrm{Re}_x)^{1/2}$, they get affected by the form of this function. In this case, the skin-friction coefficients start from fixed values and increase with increasing values of the dimensionless time. The Nusselt and Sherwood numbers also increase but at a slower rate than the skin-friction coefficients with the dimensionless time. These behaviours are clear from Figures 1–4.

The effects of the magnetic field parameter M on the velocity components in the x- and y-directions and the skin-friction coefficients for the case of a periodic fluctuating flow represented by the free stream velocity function $\phi(\tau) = (1 + \varepsilon_1 \cos \omega \tau)/(1 + \varepsilon_1)$ are depicted in Figures 5 and 6, respectively. It is observed from these figures that the presence of the magnetic field force leads to a decay of the fluid motion, so that higher rates of the fluid motion can be obtained by considering lower values of the magnetic field parameter. Moreover, for the periodic form of the function of the free stream velocity, the skin-friction coefficients take wave-like behaviours due to the presence of the function $\cos \omega \tau$ in the form of the free stream velocity. In addition, as the magnetic field parameter increases, the skin-friction coefficients increase.

Figures 7–10 illustrate the effects of the chemical reaction parameter γ on the velocity components, temperature profiles, concentration profiles, skin-friction coefficients, Nusselt number and the Sherwood number for the case of exponentially decelerating flow for which the free stream velocity function is given by $\phi(\tau) = 1 - \varepsilon_2[1 - \exp(-\varepsilon_3\tau^2)]$. It is found that, an increase in chemical reaction parameter results in a decrease in velocity components and concentration distributions whereas the temperature distributions take an opposite behaviour. On the other hand, from the third form of the free stream function we can found that the largest values of this function is 1.0 and it can be obtained by putting $\tau = 0$, so the skin-friction coefficients take the largest values at the beginning then decrease as the dimensionless time increases until they approach to zero at $\tau \to \infty$. Moreover, increasing the value of the chemical reaction parameter results in a decrease not only in the skin-friction coefficients but also in the Nusselt number whereas the Sherwood number takes the opposite behaviour.

Figures 11–14 display the effects of ratio of velocity gradients at the edge of the boundary layer c on the velocity components in x- and y-direction, temperature profiles, concentration profiles, skin-friction coefficients and Nusselt and Sherwood numbers for the case of a periodic fluctuating flow for which the free stream velocity is represented by $\phi(\tau) = (1 + \varepsilon_1 \cos \omega\tau)/(1 + \varepsilon_1)$. It is clearly observed from these figures that increasing the value of the ratio of velocity gradients at the edge of the boundary layer c leads to decreases in the fluid velocity components, temperature distribution, concentration distribution and the skin-friction coefficients whereas the Nusselt and Sherwood numbers increase.

Figures 15–18 show the effects of the heat generation/absorption parameter δ on the profiles of the velocity components in the x- and y-directions, temperature profiles, concentration profiles, skin-friction coefficients and Nusselt and Sherwood numbers for the case of periodic fluctuating flow for which the free stream velocity function is given by $\phi(\tau) = (1 + \varepsilon_1 \cos \omega\tau)/(1 + \varepsilon_1)$. From these figures we observed, as the heat generation parameter increases the velocity components of the fluid, temperature of the fluid skin-friction coefficients, Nusselt and Sherwood number decrease. However, the concentration distribution increases with increasing the heat generation parameter δ.

6 Conclusion

The problem of unsteady MHD mixed convection heat and mass transfer near the stagnation point of a 3D porous body in the presence of heat generation/absorption and chemical reaction effects was studied. The governing equations were obtained and transformed into a non-similar form. The non-similar equations were solved numerically by an efficient tri-diagonal implicit finite-difference method. Comparisons of the present results with previously published results were performed and the results were found to be in excellent agreement. From the results of the problem, we observed that

- Increasing the value of the transpiration parameter led to a decrease in the fluid velocity components and increases in both the temperature and the concentration distributions.

- In the case of a constantly accelerating flow, the skin-friction coefficients started from fixed values and increased with increasing values of the dimensionless time.

- In the case of an oscillating free stream velocity, the velocity distributions and the skin-friction coefficients responded to fluctuations in the free stream velocity.

- In the case of exponentially decelerating free stream velocity, the skin-friction coefficients decreased with increasing values of the dimensionless time.

- The heat and mass transfer characteristics were slightly affected by these free stream velocity distributions.

- The skin-friction coefficients increased as either of the transpiration parameter of the magnetic field parameter increased and decreased as either of the chemical reaction parameter, the ratio of velocity gradient parameter or the heat generation/absorption parameter increased.

- The Nusselt number increased as either of the transpiration parameter or the ratio of velocity gradient parameter increased and decreased as the chemical reaction parameter or the heat generation/absorption parameter increased.

- The Sherwood number increased as either of the transpiration parameter, the chemical reaction parameter or the ratio of velocity gradient parameter increased and decreased as the heat generation/absorption parameter increased.

References

Anjali Devi, S.P. and Kandasamy, R. (2002) 'Effects of chemical reaction, heat and mass transfer on non-linear MHD laminar boundary layer flow over a wedge with suction and injection', *Int. Commun. Heat Mass Transfer*, Vol. 29, pp.707–716.

Barenblatt, G.I. and Zel'dovich, Ya.B. (1972) 'Self-similar solutions as intermediate asymptotics', *Ado. Fluid Mech.*, Vol. 12, pp.285–312.

Bhattacharyya, S. and Gupta, A.S. (1998) 'MHD flow and heat transfer at a general three-dimensional stagnation point', *Int. J. Non-Linear Mechanics*, Vol. 33, pp.125–134.

Blottner, F.G. (1970) 'Finite-difference methods of solution of the boundary-layer equations', *AIAA J.*, Vol. 8, pp.193–205.

Chamkha, A.J. (1999) 'Hydromagnetic three-dimensional free convection on a vertical stretching surface with heat generation or absorption', *Int. J. Heat Fluid Flow*, Vol. 20, pp.84–92.

Davey, A. (1961) 'Boundary layer flow at a saddle point of attachment', *J. Fluid Mech.*, Vol. 10, pp.593–610.

Eichhorn, R. and Hasan, M.M. (1980) 'Mixed convection about a vertical surface in cross-flow: a similarity solution', *ASME J. Heat Transfer*, Vol. 102, pp.775–777.

Eswara, A.T. and Nath, G. (1999) 'Effect of large injection rates on unsteady mixed convection flow at a three-dimensional stagnation point', *Int. J. Non-Linear Mech.*, Vol. 34, pp.85–103.

Howarth, L. (1951) 'The boundary layer in three dimensional flow: part II. The flow near a stagnation point', *Philos., Meg.*, Vol. 42, p.1433.

Ishak, A., Nazar, R. and Pop, I. (2008) 'Magnetohydrodynamic (MHD) flow of a micropolar fluid towards a stagnation point on a vertical surface', *Computers and Mathematics with Applications*, Vol. 56, pp.3188–3194.

Jeng, D.R. and Williams, D.W. (1973) 'Transpiration cooling in three dimensional laminar boundary layer flows near a stagnation point', *AIAA. J.*, Vol. 11, pp.1560–1562.

Krishnaswamy, R. and Nath, G. (1982) 'Compressible boundary layer flow at a three-dimensional point with massive blowing', *Int. J. Heat Mass Transfer*, Vol. 25, pp.1639–1649.

Kumari, M. (1988a) 'Second-order boundary-layer effects for the unsteady laminar incompressible three-dimensional stagnation-point flow', *Warme-und Stoffubertragung*, Vol. 22, pp.45–54.

Kumari, M. (1988b) 'Second-order effects in unsteady laminar compressible three-dimensional stagnation-point boundary layers', *Warme-und Stoffubertragung*, Vol. 23, pp.219–227.

Kumari, M. and Nath, G. (1984) 'Unsteady free convection boundary layer flow at a three-dimensional stagnation point', *Engineering Transactions*, Vol. 32, pp.3–12.

Papenfuss, H.D. (1974a) 'Higher-order solutions for incompressible, three-dimensional boundary layer flow at the stagnation point of a general body', *Arch. Mech.*, Vol. 26, pp.981–994.

Papenfuss, H.D. (1974b) 'Mass transfer effects on the three-dimensional second-order boundary flow at the stagnation point of blunt bodies', *Mech. Res. Comm.*, Vol. 1, pp.285–290.

Papenfuss, H.D. (1977a) 'The second-order boundary-layer effects for the compressible three-dimensional stagnation-point flow', *J. Mech.*, Vol. 16, pp.705–732.

Papenfuss, H.D. (1977b) 'The second-order boundary-layer effects at the three-dimensional stagnation point with strong suction or blowing', *Z. Flugwiss. Weltraumforsch.*, Vol. 1, pp.87–96.

Prasad, A.J. and Rajappa, N.R. (1981) 'Nonsteady three-dimensional stagnation point flow with hard blowing', *ZAMM*, Vol. 61, pp.521–525.

Rahman, M.M. and Al-Lawatia, M. (2010) 'Effects of higher order chemical reaction on micropolar fluid flow on a power law permeable stretched sheet with variable concentration in a porous medium', *The Canadian Journal of Chemical Engineering*, Vol. 88, pp.23–32.

Rahman, M.M. and Salahuddin, K.M. (2010) 'Effects of variable electric conductivity and temperature dependent viscosity on magnetohydrodynamic heat and mass transfer flow along a radiate isothermal inclined surface with internal heat generation', *Communications in Nonlinear Science and Numerical Simulations*, Vol. 15, pp.2073–2085.

Rahman, M.M., Uddin, M.J. and Aziz, A. (2009) 'Effects of variable electric conductivity and non-uniform heat source (or sink) on convective micropolar fluid flow along an inclined flat plate with surface heat flux', *Int. J. Thermal Sciences*, Vol. 48, pp.2331–2340.

Ridha, A. (1990) 'Laminar mixed convection in a corner with suction', *Mech. Res. Commun.*, Vol. 17, pp.327–335.

Ridha, A. (1966) 'Three-dimensional mixed convection laminar boundary-layer near a plane of symmetry', *Int. J. Engng Sci.*, Vol. 34, pp.859–967.

Shafie, S., Amin, N. and Pop, I. (2007) 'g-Jitter free convection flow in the stagnation-point region of a three-dimensional body', *Mech. Res. Commun.*, Vol. 34, 115–122.

Sharma, P.R. and Singh, G. (2009) 'Effects of variable thermal conductivity and heat source/sink on MHD flow near a stagnation point on a linearly stretching sheet', *Journal of Applied Fluid Mechanics*, Vol. 2, pp.13–21.

Slaouti, A., Takhar, H.S. and Nath, G. (1998) 'Unsteady free convection flow in the stagnation-point region of a three-dimensional body', *International Journal of Heat and Mass Transfer*, Vol. 41, pp.3397–3408.

Vajravelu, K. and Nayfeh, J. (1992) 'Hydromagnetic convection at a cone and a wedge', *Int. Commun. Heat Mass Transfer*, Vol. 19, pp.701–710.

Vasantha, R. and Nath, G. (1986a) 'Semi-similar solution of an unsteady compressible three-dimensional stagnation point boundary layer flow with massive blowing', *Int. J. Engng. Sci.*, Vol. 23, pp.561–569.

Vasantha, R. and Nath, G. (1986b) 'Effects of large injection on unsteady compressible three-dimensional stagnation point flow', *Acta Technica CSAV*, Vol. 31, pp.177–191.

Walton, I.C. (1973) 'Boundary layer flow at a three-dimensional stagnation point with strong blowing', *Quart. J. Mech. Appl. Math.*, Vol. 26, pp.413–426.

Xu, H., Liao, S-J. and Pop, I. (2008) 'Series solutions of unsteady free convection flow in the stagnation-point region of a three-dimensional body', *Int. J. Thermal Sciences*, Vol. 47, pp.600–608.

Yao, L.S. and Catton, I. (1977) 'Buoyancy cross-flow effects on longitudinal boundary layer flow along a heated horizontal hollow cylinder', *ASME J. Heat Transfer*, Vol. 99, pp.122–124.